Inventory and recent changes of small glaciers on the northeast margin of the Southern Patagonia Icefield, Argentina

M.H. MASIOKAS,[1] S. DELGADO,[1] P. PITTE,[1] E. BERTHIER,[2] R. VILLALBA,[1] P. SKVARCA,[3] L. RUIZ,[1] J. UKITA,[4] T. YAMANOKUCHI,[5] T. TADONO,[6] S. MARINSEK,[7] F. COUVREUX,[8] L. ZALAZAR[1]

[1]*Instituto Argentino de Nivología, Glaciología y Ciencias Ambientales (IANIGLA), CCT–CONICET Mendoza, Mendoza, Argentina*
[2]*LEGOS, CNRS, Université de Toulouse, Toulouse, France*
[3]*Glaciarium, Museo del Hielo Patagónico, El Calafate, Santa Cruz, Argentina*
[4]*Department of Environmental Science, Faculty of Science, Niigata University, Niigata, Japan*
[5]*Remote Sensing Technology Center of Japan (RESTEC), Tokyo, Japan*
[6]*Earth Observation Research Center (EORC), Japan Aerospace Exploration Agency (JAXA), Ibaraki, Japan*
[7]*Instituto Antártico Argentino, Buenos Aires, Argentina*
[8]*Météo-France, CNRM/GMME/MOANA, Toulouse, France*
Correspondence: M.H. Masiokas <mmasiokas@mendoza-conicet.gob.ar>

ABSTRACT. Most glaciological studies in Argentina have focused on the large outlet glaciers of the Southern Patagonia Icefield (SPI); the numerous smaller neighboring glaciers have received significantly less attention. We present an inventory of 248 medium- to small-size glaciers (0.01–25 km^2) adjacent to the northeast margin of the SPI, describe their change over the period 1979–2005 and assess local and regional climatic variations in an attempt to explain the observed glacier changes. Based on an ASTER mosaic from 20 February 2005 and the ASTER Global Digital Elevation Model, we identified a total glacier area of 187.2 ± 7.4 km^2 between 600 and 2870 m a.s.l. Glaciers are largely debris-free and are concentrated in the western, more humid sector adjacent to the SPI. Using a 20 March 1979 US military intelligence Hexagon KH-9 satellite photograph, we measured a total areal reduction of ~33.7 km^2 (15.2%) between 1979 and 2005. Ablation season temperatures from the study area have followed a regional warming trend that could partly explain the observed glacier shrinkage. Annual precipitation estimates show a gradual decrease between 1979 and 2002 that may also have contributed to the ice mass loss.

KEYWORDS: climate change, glacier fluctuations, glacier mapping, mountain glaciers

1. INTRODUCTION

The south Patagonian Andes contain a variety of ice masses of different types and sizes which together comprise the largest glacierized area in the Southern Hemisphere outside Antarctica. The Northern and Southern Patagonia Icefields (NPI and SPI, respectively) are the largest ice masses in this region and have historically been the subject of most glaciological studies in southern South America. In Argentina, numerous studies have focused on the large outlet glaciers draining the eastern side of the SPI, but few studies have targeted the neighboring valley and mountain glaciers outside the icefield (e.g. Lliboutry, 1953; Bertone, 1960; Mercer, 1965; Röthlisberger, 1986; Popovnin and others, 1999; Masiokas and others, 2009a,b; Falaschi and others, 2013). As a result, currently there is little specific information on the location, current state or other important glaciological characteristics of these medium- to small-size glaciers, which together cover hundreds of square kilometers and a wide range of climatological conditions.

In this paper we report an inventory and analysis of recent changes of the glaciers of the Río de las Vueltas and Río Túnel hydrological basins (1435 km^2, hereafter VT basins) in the south Patagonian Andes (Fig. 1). These basins are adjacent to and immediately to the east of the SPI between Lago Viedma and Lago San Martín/O'Higgins, and contain a large number of glaciers that are two to three orders of magnitude smaller than their SPI outlet neighbors to the west. Although many of these glaciers are easily accessible from the town of El Chaltén, few detailed glaciological studies exist in the study area. We identified and mapped the glaciers in the VT basins using an excellent-quality midsummer 2005 Advanced Spaceborne Thermal Emission and Reflection Radiometer (ASTER) mosaic which has no clouds and minimum seasonal snow cover (Fig. 1). We then assessed the changes in glacier extent since 1979 using a photograph taken by the US KH-9 Hexagon spy satellite (USGS, 2008; Fowler, 2013). Interestingly, despite its great potential, the procedure for orthorectifying and co-registering these recently declassified satellite photographs has barely been used for the study of glacier changes (e.g. Pieczonka and others, 2013). The technique produced strikingly accurate co-registration of the ASTER and Hexagon images and presents promising perspectives given the medium to high spatial resolution (~10 m), extensive coverage (almost the entire SPI and adjacent areas are covered by one scene) and excellent quality of the KH-9 satellite photographs.

To explore the possible climatic forcings behind the glacier changes observed over the 1979–2005 period, we also analyzed local and regional monthly temperature and precipitation records together with gridded European Centre

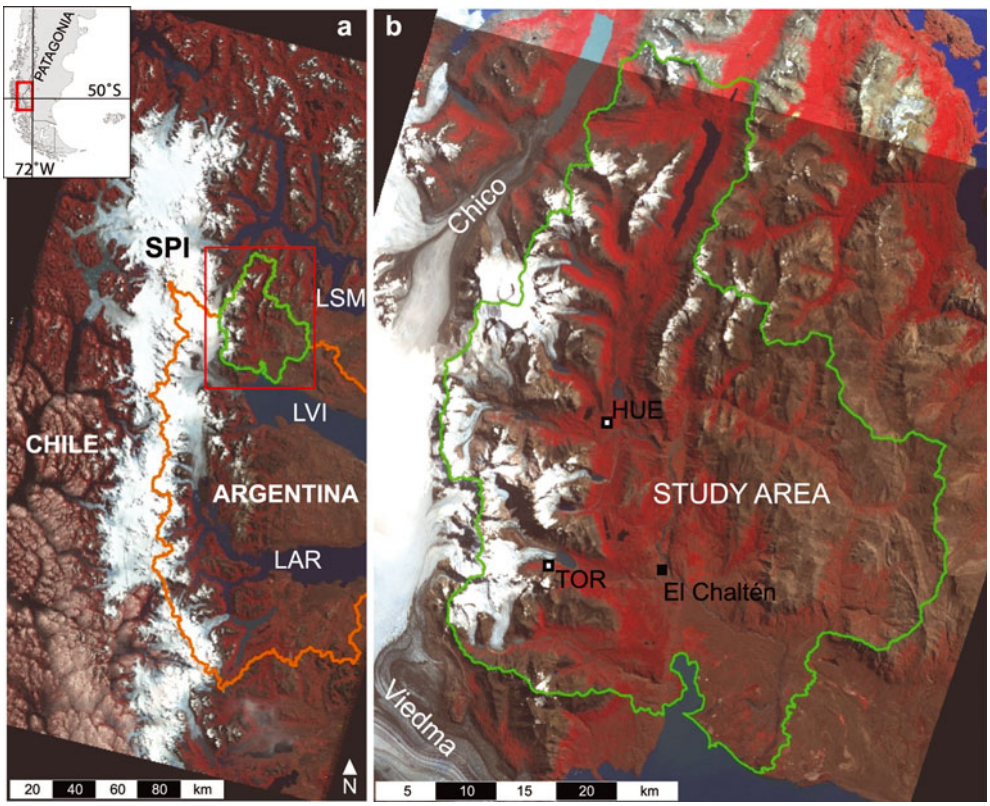

Fig. 1. (a) Mosaic (false-color composite of bands 4-3-2) of two Landsat Thematic Mapper scenes acquired on 19 February 2005 showing the location of the study area (green) on the northeastern margin of the Southern Patagonia Icefield (SPI). The limits of the upper Santa Cruz river basin (orange) and the lakes San Martín/O'Higgins (LSM), Viedma (LVI) and Argentino (LAR) are also shown. Collectively, this portion of the Andes contains the largest glaciated area in Argentina. (b) Closer view of the study area as observed on a mosaic (false-color composite of bands 3-2-1) of two Terra ASTER scenes acquired on 20 February 2005. The glaciers Chico and Viedma are shown to illustrate the differences between these large SPI outlet glaciers and the significantly smaller ice masses analyzed in this study. The town El Chaltén and the location of the Torre temperature data logger (TOR) and the Estancia Los Huemules precipitation station (HUE) are also indicated.

for Medium-Range Weather Forecasts ERA-Interim reanalysis data (Dee and others, 2011). Some of the surface climate records are short and/or incomplete but were included in the analyses because they provide direct, previously unpublished climatic information from this data-poor region. The analyses were carried out as part of the ongoing National Glacier Inventory project, which aims to develop a complete and well-documented inventory of glaciers and ice-rich periglacial features (rock glaciers) in the Argentinian portion of the Andes, with regular updates every 5 years. The results provide important new data for this area that could be useful for regional and larger-scale assessments of glacier–climate linkages and glacier variations throughout the Andes.

2. PREVIOUS STUDIES

Bertone (1960) presented preliminary information on the area and state of 356 glaciers in the Argentinian Andes between 47°30′ S and 51° S based on aerial photographs from 1944–45 and field surveys conducted in the 1950s. Unfortunately, the reported glacier areas have large uncertainties which are not particularly useful for comparison with current glacier extents. Subsequent studies have reported more accurate inventory information for the glaciers in this region, but, as mentioned above, they have focused on the larger outlet glaciers draining the Patagonian icefields (e.g. Aniya, 1988; Aniya and others, 1996; Skvarca and De Angelis, 2003). Recently, Pfeffer and others (2014) presented the Randolph Glacier Inventory (RGI; available through the Global Land Ice Measurements from Space (GLIMS) website www.glims.org/RGI/randolph.html), the first global glacier inventory developed through the coordinated effort of a large number of glaciologists. Although the RGI includes outlines of thousands of glaciers in the southern Andes, many smaller-scale features and debris-covered sectors of glaciers may remain poorly represented until more accurate local or regional inventories become available and are incorporated into the database (Pfeffer and others, 2014).

Davies and Glasser (2012) presented a comprehensive assessment of glacier changes in the Patagonian Andes since the peak of the Little Ice Age (LIA) using trimlines and moraines. In agreement with several previous studies (e.g. Masiokas and others 2009b and references therein), Davies and Glasser (2012) showed that the vast majority of glaciers in the Patagonian Andes have experienced a noticeable ice mass loss since the LIA, with a possible increase in the retreat rates in recent years (see also Rignot and others, 2003; Willis and others, 2012).

Unfortunately, the sparse distribution of meteorological stations and the unknown quality and uneven temporal coverage of available records hamper detailed assessments of recent climatic trends and glacier–climate interactions in southern Patagonia. Earlier studies interested in the spatio-temporal climatic variability in this region usually relied on a similar, small set of stations containing the longest and most complete records (e.g. Rosenblüth and others, 1995,

Table 1. Satellite images used in the development of the glacier inventory of the VT basins

Satellite/sensor	Image ID	Date	Pixel resolution m	Use
Terra/ASTER*	AST_L1A.003:2028179509 AST_L1A.003:2028179492	20 Feb 2005	15	2005 glacier inventory
Landsat 7/ETM+	L71231094_09420050227	27 Feb 2005	30	Base for geo-referencing
Landsat 5 /TM	LT5231094_2005050COA00	19 Feb 2005	30	Support for identification and mapping of features
Landsat 7/ETM+	L71231094_09420080119	19 Jan 2008	30	Support for identification and mapping of features
ALOS/PRISM	ALPSMN116044595	29 Mar 2008	2.5	Support for identification and mapping of features
KH-9 Hexagon/9-inch film camera	ID DZB1215–500030L001001	20 Mar 1979	6–9	1979 glacier inventory

*The 2005 ASTER scenes were provided as On-demand Level-3 Orthorectified Image products (https://lpdaac.usgs.gov/products/aster_products_table/ast14oth).

1997; Carrasco and others, 2002; Villalba and others, 2003; Aravena and Luckman, 2009). These studies indicate an overall 20th-century warming and varying precipitation trends for different stations in southern Patagonia, providing useful but limited evidence for a proper assessment of the climatic causes behind the glacier shrinkage observed in recent decades. Recently, the integration of reanalysis datasets with regional and local downscaling exercises has substantially improved the spatial coverage and temporal resolution of the climatic information available for Patagonian glaciers (e.g. Rasmussen and others, 2007; Garreaud and others, 2013; Schaefer and others, 2013, 2015; Lenaerts and others, 2014). These newer datasets have allowed, for example, the calculation of surface mass-balance estimates for the entire SPI since the mid- to late 1970s, and will likely represent a crucial resource in future studies of glacier–climate interactions and glacier dynamics in this data-poor region (Lenaerts and others, 2014; Schaefer and others, 2015). However, in order to validate the results and reduce the uncertainties associated with these large-scale, promising modeling exercises, localized glaciological and meteorological measurements together with detailed assessments of recent glacier changes are still needed in many sectors of the Patagonian Andes.

3. DATA AND METHODS

3.1. Study area

The study area is located near 49°19′ S, 72°55′ W in the province of Santa Cruz, southwestern Argentina (Fig. 1). It includes the Río de las Vueltas and Río Túnel hydrological basins and the northeast portion of the SPI. These basins are part of the extensive Río Santa Cruz hydrological system which drains the eastern side of the SPI into the South Atlantic Ocean. This sector of the Patagonian Andes is characterized by steep environmental gradients between the extremely humid conditions on the SPI and the arid Patagonian steppe only a short distance to the east (Carrasco and others, 2002; Villalba and others, 2003). Given this rare combination of environmental conditions and features, this region has long been recognized as an important site for glaciological studies (Kölliker and others, 1917; Mercer, 1965; Warren and Sugden, 1993; Casassa and others, 2002). The ice masses in the study area are mostly clean-ice, small glaciers with a few debris-covered sectors.

3.2. Satellite imagery

Given the characteristics of the glaciers in the study area, their detection and mapping from remote sensors is relatively straightforward using a set of well-documented techniques (e.g. Racoviteanu and others, 2009). The main limitation for inventorying these glaciers is the lack of good-quality, cloud-free images for this region. Indeed, a search through the database of medium-resolution (15 m) Terra ASTER scenes revealed very few images suitable for glacier inventory purposes in the study area. We selected two scenes acquired in the 2005 austral summer (20 February 2005; Table 1) which were virtually cloud-free and contained almost no seasonal snow cover outside the glacier margins. In order to maintain a consistent co-registration with inventories from adjacent basins (Fig. 1a), we co-registered the ASTER images with a Landsat Enhanced Thematic Mapper Plus (ETM+) scene from 27 February 2005, and then built a mosaic from the two scenes (Table 1; Fig. 1b). Additional cloud-free Landsat scenes with minimum seasonal snow coverage were used as complementary images during the digitization of the glacier outlines and to differentiate seasonal from permanent snowpatches (Table 1). We also used an ALOS-PRISM (Advanced Land Observation Satellite, Panchromatic Remote-sensing Instrument for Stereo Mapping; Tadono and others, 2009) 2.5 m pixel resolution scene from 29 March 2008, which covers the eastern portion of the study area, to better identify a set of small rock glaciers and snowpatches on this drier sector. Unfortunately, no suitable ALOS scenes were available for the western portion of the study area where most of the glaciers are located. We used the 30 m resolution Global Digital Elevation Model derived from the Terra ASTER sensor (GDEM v2; hereafter GDEM; Frey and Paul, 2012) to facilitate the identification of the main hydrological basins together with the sub-basins and ice divides within them.

3.3. Glacier identification and mapping

Glaciers and permanent snowpatches larger than 0.01 km^2 (1 ha) in size were identified and their outlines delimited following the recommendations of the GLIMS expert panel (Racoviteanu and others, 2009). Clean ice and snowpatches were initially detected semi-automatically calculating a band ratio between ASTER bands 3N and 4 and applying a masking threshold of 1.1 selected interactively (i.e. band

Table 2. Surface temperature and precipitation records used in this study. Data sources: GHCN: Global Historical Climatology Network; DMC: Dirección Meteorológica de Chile; IANIGLA: Instituto Argentino de Nivología, Glaciología y Ciencias Ambientales; DGA: Dirección General de Aguas, Chile; SSRH: Subsecretaría de Recursos Hídricos, Argentina; SMN: Servicio Meteorológico Nacional, Argentina

Station (source)	ID in figs	Lat., long., elev. °S, °W, m	Period (% missing)	Variable
Balmaceda (GHCN)	1	45.9, 71.7, 520	1961–2005 (0.6)	Temp.
Chile Chico (DMC)	2	46.5, 71.7, 327	1965–2001 (5.4)	Temp.
Cochrane (DMC)	3	47.2, 72.5, 182	1969–2001 (2.6)	Temp.
Lago Argentino (GHCN)	4	50.3, 72.3, 220	1961–2005 (1.5)	Temp.
Río Gallegos (GHCN)	5	51.6, 69.3, 19	1931–2005 (6.7)	Temp.
Punta Arenas (GHCN)	6	53.0, 70.8, 37	1888–2005 (1.0)	Temp.
Ushuaia (GHCN)	7	54.8, 68.3, 14	1901–2005 (4.8)	Temp.
Glaciar Torre (IANIGLA)	TOR	49.33, 73.01, 885	2002–12 (0)	Temp.
Villa O'Higgins (DGA)	VHO	48.47, 72.56, 270	1993–2008 (16.1)	Precip.
Estancia Entre Ríos (SSRH)	EER	48.26, 72.22, 480	1980–2014 (13.1)	Precip.
Puerto Edén (DGA)	EDE	49.12, 74.41, 10	1997–2011 (25)	Precip.
Candelario Mancilla (DGA)	CAM	48.88, 72.74, 300	1994–2012 (37.7)	Precip.
El Chaltén (SSRH)	CHA	49.34, 72.86, 385	1983–2014 (13.3)	Precip.
Lago Argentino (SMN)	LGA	50.3, 72.3, 220	1936–2000 (1.7)	Precip.
Estancia Los Huemules (personal communication)	HUE	49.22, 72.96, 460	2006–14 (0)	Precip.

3N/band 4 > 1.1 = ice + snow). Then the outlines of all ice masses were carefully examined on the screen and manually corrected to include debris-covered ice or ice in cast shadows, and to exclude misclassified sectors resulting from the semi-automated band ratio approach. The mapping was initially performed by two operators and subsequently submitted for review and approval by a glaciologist with a thorough knowledge of the glaciers in this area. The final inventory map incorporates the corrections suggested by this external expert reviewer. Based on their morphological characteristics, each ice body was classified according to the guidelines used in the National Glacier Inventory project (IANIGLA, 2010). These guidelines are based on those originally proposed by the World Glacier Monitoring Service and GLIMS programs, with some modifications to incorporate different types of rock glaciers into the dataset. The calculation of glacier areas was complemented with additional basic measurements such as the length, orientation and elevation range of each glacier. Whenever possible, the location and elevation of the transient snowline was determined visually based on the ASTER scene and 50 m contours derived from the digital elevation model.

3.4. Changes 1979–2005

A recently declassified 10 m resolution photograph from the US military intelligence KH-9 Hexagon satellite acquired on 20 March 1979 (Table 1; Fowler, 2013) was used to measure glacier changes in the study area over the 1979–2005 period. To allow a direct comparison with the 2005 ASTER base images, the 1979 photograph was first resampled to a pixel size of 15 m and then orthorectified and co-registered using COSI-Corr (Co-registration of Optically Sensed Images and Correlation), a freely available plug-in for the ENVI Exelis software (Leprince and others, 2007). The procedure for processing the KH-9 photograph with COSI-Corr is discussed in Hollingsworth and others (2012) and also in the COSI-Corr forum (http://tecto.gps.caltech.edu/forum/viewtopic.php?id=101). The orthorectification was performed using 12 tie points selected between the ASTER mosaic and the KH-9 photograph. Visual examination of the two images showed that a slight horizontal shift remained in the 1979 photograph after orthorectification. A cross-correlation of the two images over stable areas (i.e. excluding glaciers and lakes) showed that the KH-9 photograph had a mean shift of 5 m to the north and 15 m to the west. These shifts were applied to the KH-9 image and resulted in an excellent co-registration with the ASTER base image.

After enhancing the 1979 photograph using a 2% linear contrast stretch, each glacier and snowpatch with an area $\geq$0.01 km^2 (1 ha) was mapped manually, paying special attention to sectors in shadow and/or containing debris-covered ice. The vector files containing the glacier boundaries were examined by two reviewers and subsequently used to estimate areal changes of the glaciers over the 1979–2005 period. Since there were no high-resolution images available for the same time period for comparison, we estimated the uncertainty in the 1979 and 2005 areas assuming an error of one pixel over the entire perimeter of the glaciers. This approach offers an objective error estimate in this area with a predominance of relatively easy-to-identify clean-ice glaciers. Finally, flowlines of mountain and valley glaciers initially identified on the 2005 image were superimposed on the KH-9 photograph and extended to the 1979 glacier front positions to estimate glacier length changes over the 1979–2005 interval.

3.5. Climatic trends

Monthly temperature data from several official weather stations (Table 2) were used to assess the possible climatic causes behind the recent glacier changes. As none of these official stations is located inside the study area (the closest station with >15 years of record, Lago Argentino near El Calafate, is >100 km southeast of El Chaltén), we also included in the analyses 2002–12 data from a HOBO temperature data logger (hereafter TOR) located at 885 m a.s.l. near the upper treeline on the north-facing slope adjacent to Glaciar Torre (Fig. 1; Table 2), and mean monthly gridded surface temperature data from the ERA-Interim reanalysis dataset (Dee and others, 2011). This gridded dataset has 0.75° × 0.75° spatial resolution and is available since January 1979. ERA-Interim surface precipitation data were

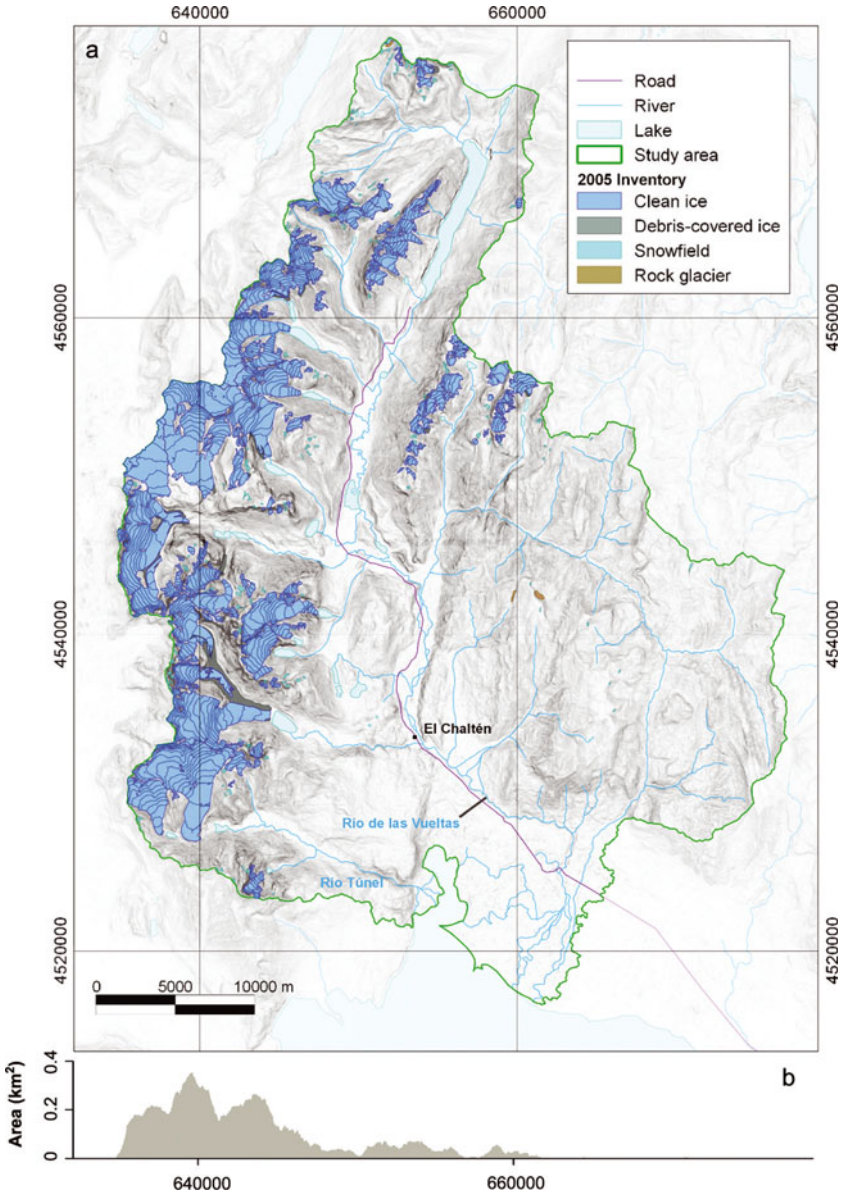

Fig. 2. (a) Map showing the glacier inventory of the VT hydrological basins based on an ASTER mosaic from 20 February 2005 (map projection UTM 18S, datum WGS84). The town of El Chaltén is located at ~49°19′44″ S, 72°55′48″ W (450 m a.s.l.). (b) Distribution of glaciated area vs longitude in the study area. Note the concentration of glaciers towards the western, most humid sectors adjacent to the SPI.

also used for comparison with monthly total precipitation records collected at several stations inside or in the vicinity of the study area (Table 2). The use of these gridded datasets allowed the assessment of the spatial representativeness of the station records and also the identification of local temperature and precipitation patterns to characterize recent variations in the study area.

4. RESULTS

We identified 248 ice masses with a total area of $187.2 \pm 7.4\,km^2$ in the VT basins in 2005 (Fig. 2a). This represents ~13% of the total area ($1435\,km^2$) of these hydrological basins. The glaciers range from $0.01\,km^2$ to almost $25\,km^2$ in area, with an average size of $0.75\,km^2$. The largest glaciers (Glaciar Torre ($24.66\,km^2$), Glaciar Gorra Blanca ($17.12\,km^2$) and Glaciar Túnel ($16.99\,km^2$)) and most of the glaciated area inventoried here are located in the western portion of the study area, with the size of the ice masses decreasing markedly towards the eastern, drier sectors of the VT basins (Fig. 2b). The predominance of clean-ice glaciers is apparent in Figure 3a: almost 95% of the inventoried area was classified as clean ice, with debris-covered ice and permanent snowfields/glacierets accounting for the remaining 3% and 2%, respectively. Only three small rock glaciers, with $\sim 0.35\,km^2$ of total surface area (0.18% of the inventory), were identified in these basins. The frequency distribution of glacier sizes is dominated by small ice masses (Fig. 3b). Two hundred and eighteen units (87.9% of the total) are $<1\,km^2$ in size, 19 glaciers (7.6%) are between 1 and $5\,km^2$, and only 11 glaciers (4.4%) are $>5\,km^2$ in surface area. The smaller ($<1\,km^2$) units are by far the most numerous but account for only 13% ($24.45\,km^2$) of the total glaciated area, whereas the 30 largest ($>1\,km^2$) glaciers represent ~87% ($162.74\,km^2$) of the inventoried surface (Fig. 3b).

The glaciers in the study area cover an altitudinal range of ~2300 m, with the highest point at 2868 m a.s.l. and the lowest glacier terminus at 600 m a.s.l. (Fig. 3c). Within this range, the largest concentration of glacier ice occurs

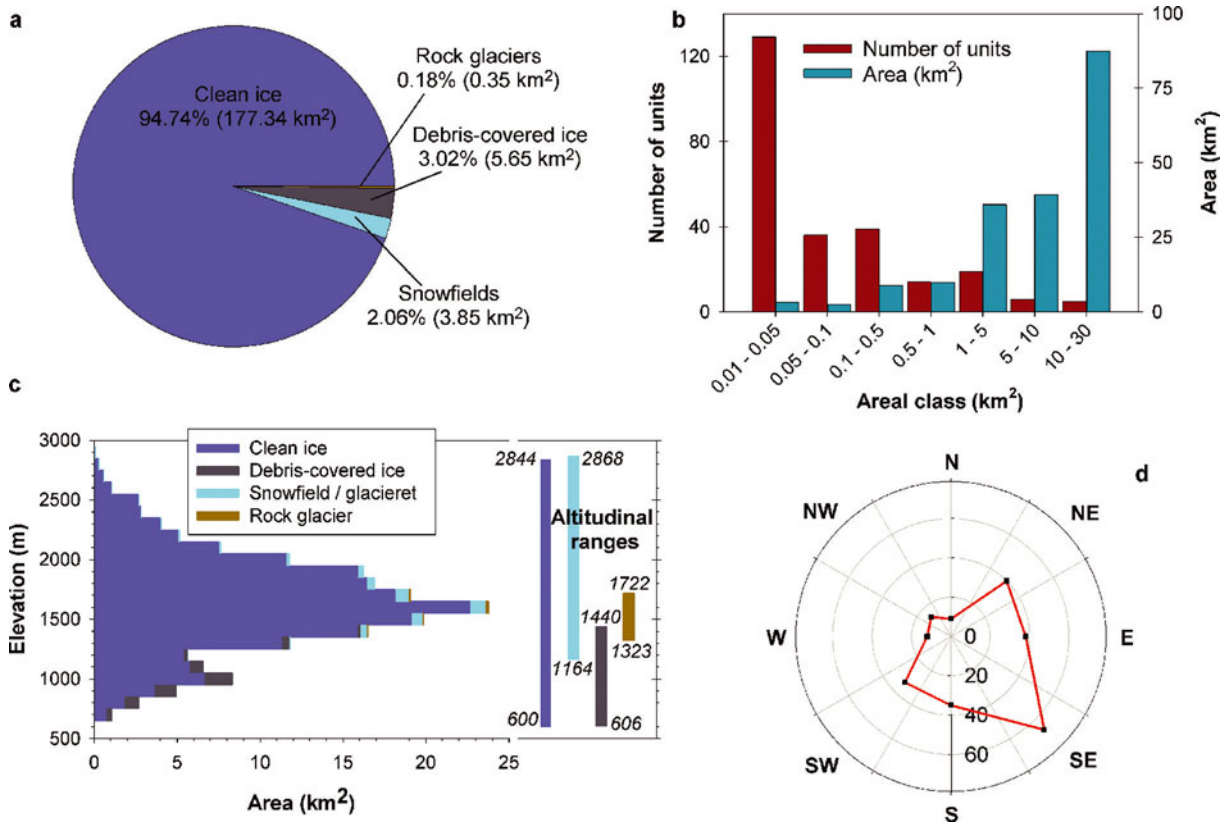

Fig. 3. (a) Percentage of total inventoried area of the different types of geoforms identified in this study. (b) Number of units and surface area covered by these units, grouped by size. Note that the smallest units are the most numerous but cover a relatively small surface area, whereas the largest glaciers are only a few but occupy the bulk of the area. (c) Hypsometry of the different surface types inventoried in the study area. Note the predominance of clean ice, mostly concentrated between 1300 and 2000 m, and the existence of debris-covered ice only at low elevations. (d) Orientation of the units inventoried in the VT basins.

between 1300 and 2000 m a.s.l. Clean ice surfaces cover the widest altitudinal range, between 600 and 2844 m a.s.l. Although covering a relatively small surface area, glacierets and permanent snowfields are also distributed along a wide altitudinal range, between 1164 and 2868 m a.s.l. In contrast, debris-covered ice is only found at lower elevations (between 606 and 1440 m a.s.l.) on the snouts of some glaciers (Figs 2 and 3c). The few rock glaciers identified in this area occupy a limited altitudinal range, between 1323 and 1722 m a.s.l. The majority of the glaciers have a southeastern orientation, with a smaller proportion of units oriented towards the south, east, southwest and northeast (Fig. 3d). This pattern is consistent with glaciers being located on the colder and less illuminated slopes in the Southern Hemisphere. Very few glaciers are oriented towards the north, northwest and west. The position of the transient snowline was easily identifiable in ~25% of the inventoried units (64 glaciers; figure not shown). On these glaciers, the 20 February 2005 snowline ranges from 1250 to 1950 m a.s.l., with an arithmetic mean of 1600 m a.s.l. and a standard deviation of 160 m.

Using the KH-9 photograph as a reference, we identified 229 ice masses covering a total area of 220.89 ± 7.41 km^2 and with an average size of 0.99 km^2. Comparison with the 2005 values indicates that the total areal reduction between 1979 and 2005 is ~33.7 km^2 (15.2%). Figure 4a shows an oblique three-dimensional (3-D) view of part of the KH-9 image with the position of the glacier margins in 1979 and 2005. An analysis of areal changes vs elevation (Fig. 4b) indicates that the larger ice losses occurred at around 1200–1600 m a.s.l. Area losses observed below these elevation bands are only marginally lower and can also be observed at higher elevations, indicating a generalized glacier reduction throughout the altitudinal range (Fig. 4b). Within the overall pattern of glacier recession observed during the 1979–2005 interval, we find that the relative reduction of the different units is highly dependent on glacier size and location (Fig. 5). In terms of areal change, the smaller units show a much wider range of variability than the larger glaciers, with some small units losing 100% of their 1979 area by 2005 and others showing virtually no change over this interval (Fig. 5a). The 1979–2005 relative reduction of the units $\geq$1 km^2 is more homogeneous and ranges between 10% and 30%. Length changes of mountain and valley glaciers (97 units in total) display a similar pattern. The smaller glaciers show a wider spread ranging between 0 and 40% of shortening with respect to their length in 1979. The longer units ($\geq$2000 m) show a more homogeneous pattern with ~10% of relative reduction between 1979 and 2005 (Fig. 5b). In relative terms, the largest areal losses are concentrated in the eastern sector of the study area (Fig. 5c). Several of the small ice masses identified in 1979 in this drier sector had disappeared by 2005, and in general the percent reduction is substantially larger than that observed towards the more humid western sector of the VT basins.

Mean monthly temperature variations at TOR show strong positive correlations with local and regional gridded ERA-Interim surface temperatures between 2002 and 2012 (Fig. 6a). On a local scale, the highly significant correlation between TOR and the ERA-Interim gridcell centered at the

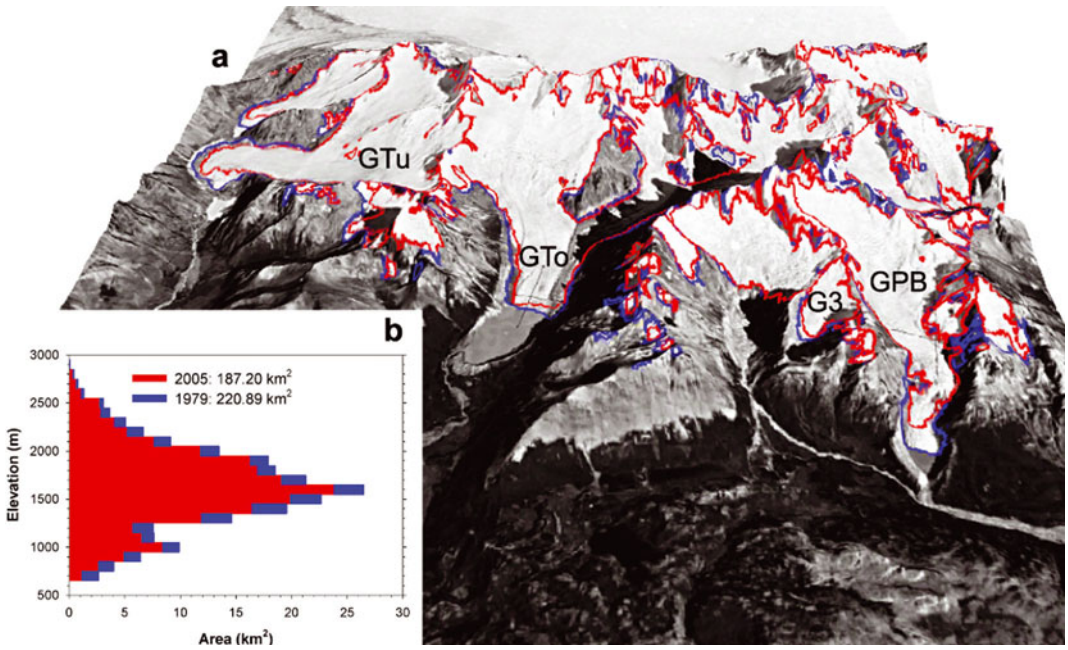

Fig. 4. (a) Oblique view of a portion of study area showing the glacier margins in 1979 and 2005 (blue and red, respectively). The 3-D effect was created by overlaying the KH-9 image on the GDEM. Some of the best-studied glaciers are indicated: Torre (GTo), Túnel (GTu), de los Tres (G3) and Piedras Blancas (GPB). (b) Changes of glaciated area vs elevation between 1979 and 2005 (blue and red bars, respectively).

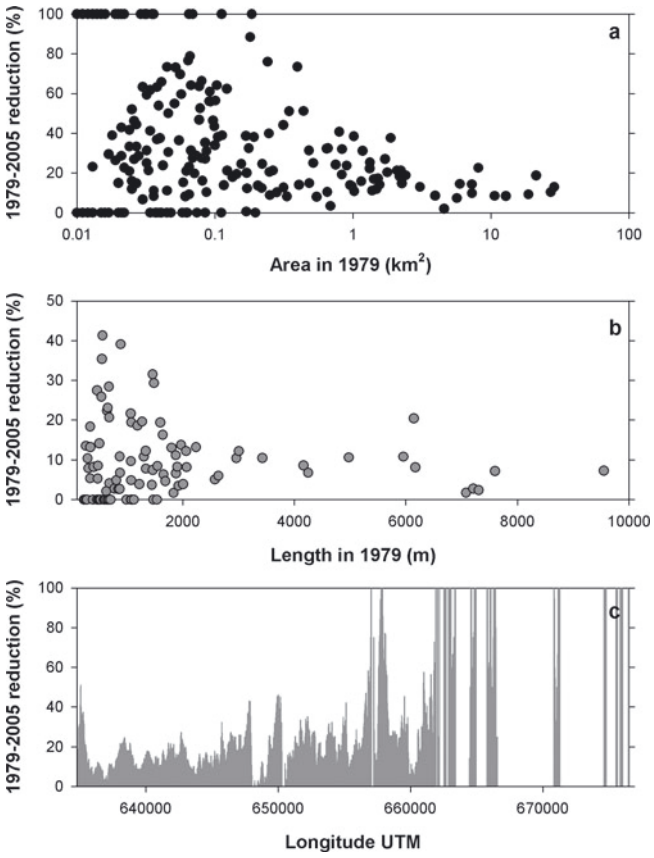

Fig. 5. (a) Changes in area of the glaciers inventoried in the VT basins between 1979 and 2005. The changes are indicated as a percent reduction using the 1979 areas as a reference. (b) Same as (a), but for the length of 97 mountain and valley glaciers identified in the study area. Note that the smaller units show a larger variability in both areal and frontal changes. (c) Same as (a), but showing the relative areal changes of glaciers based on the longitude. The complete disintegration (100% reduction) of ice masses only occurred in the eastern half of the study area.

study area (gridcell centered at 49° S, 73° W; Fig. 6b) provides solid evidence of the reliability of these independent datasets. The strong correlation between these records also offers the opportunity to reconstruct the short TOR series using the longer gridded reanalysis data. The result of this analysis is depicted in Figure 6c, where the 2002–12 TOR mean monthly temperature data are estimated through simple linear regression using the 1979–2014 local gridcell reanalysis series as predictor. On a regional scale, the pattern of strong positive correlations between TOR and ERA-Interim data extends to all land areas south of 44° S and also towards the southeast Pacific Ocean several hundreds of kilometers from the continent (Fig. 6a). All of the official surface temperature stations listed in Table 2 are located within this extensive area of positive correlations, suggesting an important percentage of common variance in these south Patagonian records. This is corroborated in Figure 7a, which includes a regionally averaged series of October–March (ablation season) mean temperatures of the seven stations in Table 2, together with observed and predicted October–March mean temperatures at TOR (Fig. 6b). Evaluated in a longer-term context, between 1931 and 2005 the regional temperature record shows a gradual warming trend interrupted by at least two clear cooling periods in the early to mid-1970s and in the first years of the 21st century (Fig. 7a). Between 1979 and 2005 the study area experienced relatively warm conditions in the 1980s and early 1990s, much cooler years between 2000 and 2003, and a marked jump towards higher temperatures in 2004–05 (Fig. 7a). The conditions in 2005 are among the warmest recorded and predicted for this area, and likely influenced the (minimal) snow coverage observed in the 20 February 2005 ASTER image used to inventory glaciers in this study.

The field correlations between the monthly total precipitation series in Table 2 and the gridded ERA-Interim data indicate that most station records are strongly and positively correlated with local reanalysis gridcells (Figs 8 and 9a).

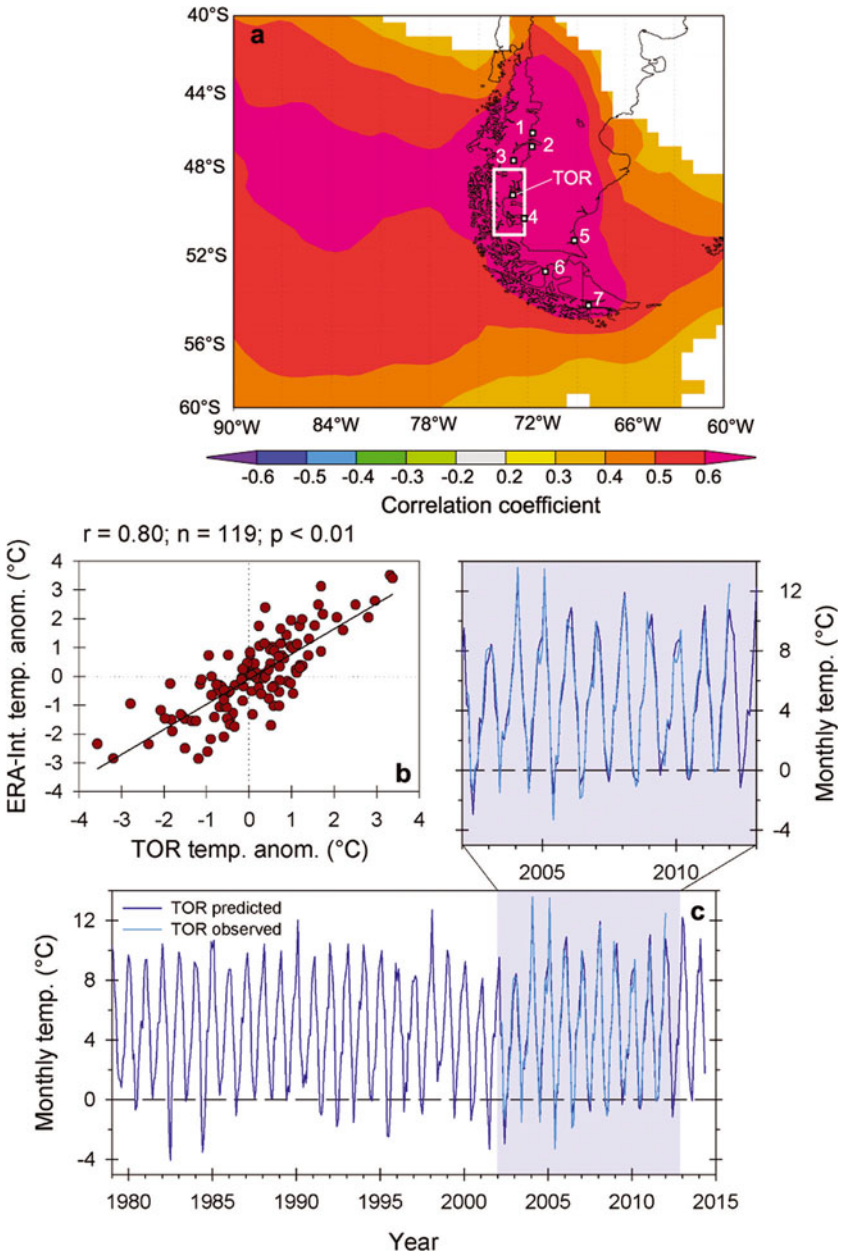

Fig. 6. (a) Field correlations between gridded ERA-Interim mean monthly surface temperature data and the records collected at the Glaciar Torre data logger (TOR) between 2002 and 2012. Only statistically significant correlations ($p < 0.05$) are shown. Prior to computing the correlations, the series were converted to temperature anomalies by subtracting their seasonal cycle. The extent covered by Figure 1a is shown by a rectangle, and the location of other temperature stations in southern Patagonia is also indicated (see Table 2). (b) Scatter plot showing the strong positive correlation between mean monthly surface temperature anomalies at the ERA-Interim gridcell centered at 49° S, 73° W and those observed at TOR. (c) Mean monthly temperature variations recorded and predicted at TOR (light and dark blue, respectively). TOR monthly temperature anomalies over the 1979–2014 period were first estimated through simple linear regression using the 49° S, 73° W ERA-Interim gridcell values as predictors, and then converted back to mean monthly values using the seasonal cycle observed at TOR between 2002 and 2012.

These figures show that in general the areas of strongest co-variability are restricted to few adjacent gridcells and tend to extend to the north and northwest of the stations' locations. The low correlations observed in the case of the El Chaltén series (a potentially useful record as it is the longest precipitation series available in the study area) suggest that this record contains errors (Fig. 8e). In contrast, the precipitation record from Lago Argentino near El Calafate shows relatively strong correlations with local reanalysis gridcells (Fig. 8f), but this association concentrates on the Patagonian steppe and does not extend towards the west where glaciers are located. In Figure 9a we focus on the relationship between ERA-Interim precipitation data and monthly precipitation totals from Estancia Los Huemules (HUE; Table 2; Fig. 1). The HUE record covers a significantly shorter period than other stations listed in Table 2 but has the advantage of being located only a few kilometers from the glaciers in the VT basins. Based on the strong positive correlation between this series and the monthly precipitation data in the ERA-Interim gridcell centered at 49° S, 73° W (Fig. 9b), we developed a simple linear regression model and estimated monthly precipitation variations at HUE back to January 1979 (Fig. 9c). The aggregated April–March (glaciological year) totals derived from this reconstructed series (Fig. 7b)

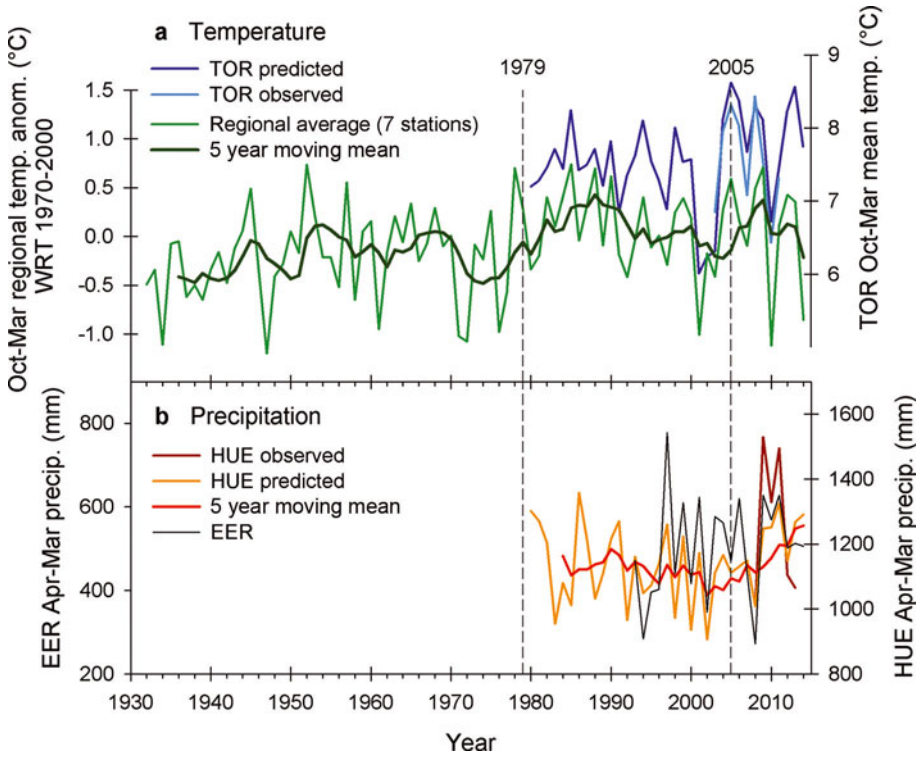

Fig. 7. (a) October–March mean temperature variations as recorded and predicted for TOR (light and dark blue, respectively). A regionally averaged October–March mean temperature series derived from the seven longest station records available in southern Patagonia (light green; Table 2) is also included for comparison. Prior to computing this regional composite series, monthly records from these stations were averaged into October–March seasonal values and expressed as anomalies from the mean of the 1970–2000 period common to all series. The series starts in 1931 when at least three station records are available to compute the regional series. Missing values were excluded from the computation of this regional average. Five-year moving averages plotted at the latest year of each moving window are shown to emphasize the low-frequency patterns in this record. (b) April–March precipitation totals observed and predicted for HUE (brown and orange, respectively; see Fig. 9). The 5 year moving averages of the predicted HUE series are shown in red. The April–March precipitation totals for Estancia Entre Ríos (EER, black) are also shown for comparison. This record starts in 1980, but prior to 1992 it contains a large percentage of missing data that precluded the calculation of annual precipitation totals.

show a gradual decrease in precipitation until 2002 followed by an increasing trend which has continued up to the present. The series from Estancia Entre Ríos (EER; Table 2; Fig. 8b) is the only complete, well-correlated station record longer than a decade in the vicinity of the VT basins. Aggregated into April–March totals (Fig. 7b), the EER and HUE series (observed and predicted) show a similar pattern of variations which indicates that these records can be considered representative of recent precipitation variations in the study area.

5. DISCUSSION

In this contribution we provide new inventory information for 248 ice masses (ranging between 0.01 and 25 km^2 in size and covering a total area of 187.2 ± 7.4 km^2) located in the VT hydrological basins on the northeast margin of the SPI (Figs 1 and 2). These basins are part of the Río Santa Cruz hydrological system, the largest river draining to the Atlantic in Patagonia. The inventory information was obtained following well-documented international guidelines for mapping glacier ice from satellite imagery, adapted and expanded to conform to the particular requirements of the ongoing National Glacier Inventory in Argentina. In addition to the inventory data for each glacier, we also determine their hypsometry and several other parameters to contribute to the understanding of the glaciated area in these basins. Although glacier ice is found at elevations ranging between 600 and 2780 m a.s.l., the glaciated area in these basins is largely concentrated within the 1300–2000 m a.s.l. altitudinal range (Fig. 3). A clear predominance of clean-ice surfaces (covering almost 95% of the inventoried area) is a salient characteristic of this inventory. Glaciers in the study area show a remarkable contrast in size and distribution, with large adjacent glaciers in the west and small, disperse snowfields and glacierets only a few km to the east (Fig. 2). These differences are largely determined by a steep precipitation gradient which ranges from several meters of annual precipitation on the SPI to 100–200 mm on the Patagonian steppe (Carrasco and others, 2002; Villalba and others, 2003; Lenaerts and others, 2014). We only identified a few debris-covered sectors (~3% of the total area) on the lower, terminal portions of some glaciers (Figs 2 and 3), and three small rock glaciers (the largest has an area of 0.18 km^2 and is ~700 m long) in the drier sector of the VT basins. This is markedly different to the results of similar studies performed farther north in the drier, central Andes of Argentina (~32° S), where debris-covered glaciers and rock glaciers constitute a large proportion (>50%) of the inventoried surfaces (e.g. Zalazar and others, 2012). Although not important in terms of total area, the existence of rock glaciers (Barsch, 1996) so far south in the Andes provides interesting new evidence for comparison with other drier areas farther north and contributes to a more comprehensive understanding of the glacial and periglacial environments in this region.

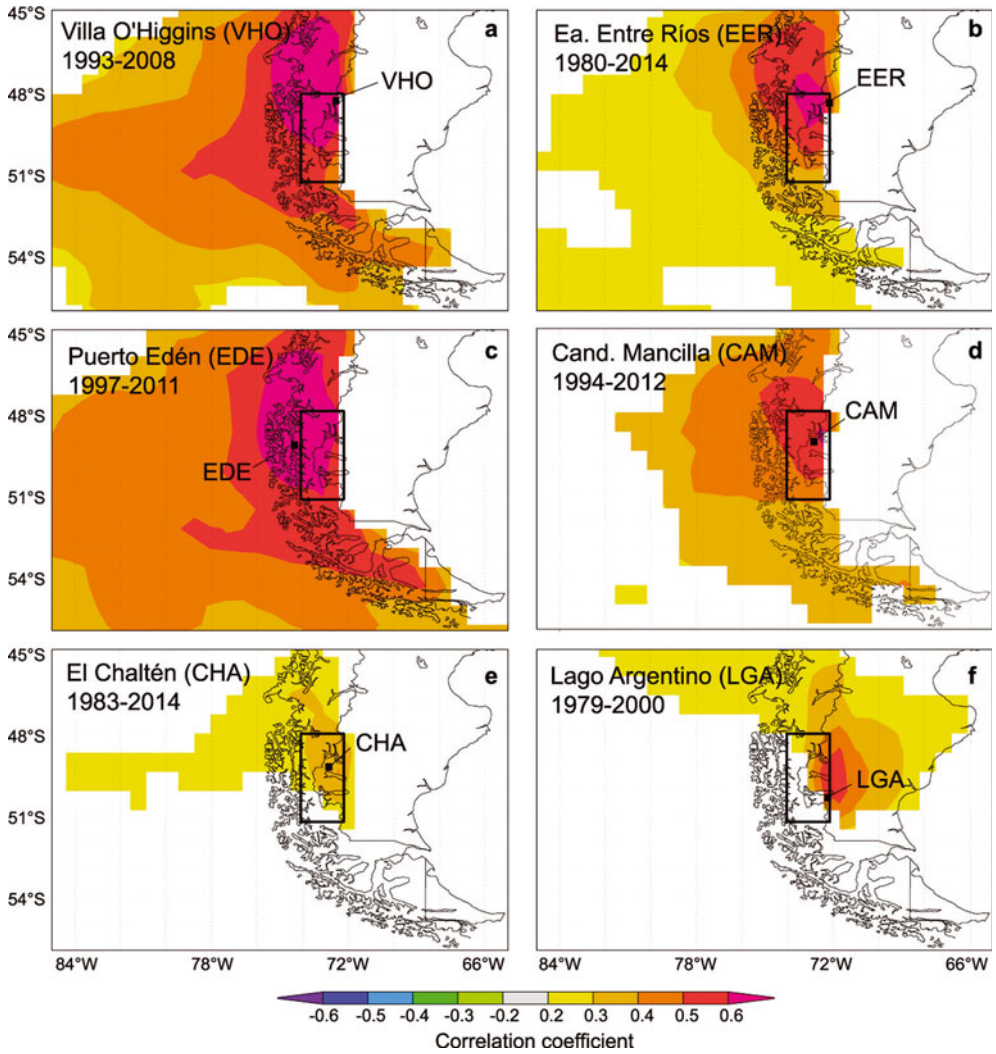

Fig. 8. Field correlations between gridded ERA-Interim monthly surface precipitation data and selected station records (see Table 2). Only statistically significant correlations ($p < 0.05$) are shown. Prior to computing the correlations, all gridded and station series were converted to precipitation anomalies by subtracting their seasonal cycles. Missing values were not considered in the correlations. In each panel the extent covered by Figure 1a is shown by a rectangle together with the location of the station and its period of overlap with the reanalysis data.

Between 1979 and 2005, the VT glaciers lost ~15.2% (33.7 km^2) of their surface area. The magnitude of recession is, however, quite variable and depends on the size and location of the units, with smaller glaciers showing a rather wide range of shrinkage (0–100%) and the larger units a more consistent pattern varying around 10–20% of areal reduction since 1979 (Fig. 5a). The analyses also show that all the ice masses that disappeared between 1979 and 2005 were concentrated in the eastern drier half of the study area (Fig. 5c). During field surveys we have observed that some glaciers which have experienced relatively small areal reductions over recent decades (e.g. Glaciar Torre; Fig. 4a) have shown nonetheless a clearly visible downwasting of the glacier surface. This suggests that glacier mass losses are proportionally greater than the areal estimates discussed here indicate. We also note a different number of units identified in 1979 and 2005 (229 vs 248 units, respectively), which results from the disintegration of some ice masses into a group of smaller units. This represents further evidence of the generalized glacier wastage reported for this area over this 26 year period.

Surface temperature variations throughout southern Patagonia share a large percentage of common variance and show a long-term warming trend that could be partly responsible for the generalized glacier retreat observed in the region (Figs 6 and 7a). The local and regional records developed here suggest, however, that temperatures in this region have not increased monotonically. Prior to 2005, the warming tendency is largely driven by higher than normal temperatures between the late 1970s and the early 1990s and also in 2004–05, when local ablation season temperatures probably reached one of the highest levels in recent decades (Fig. 7a). Cooler than normal conditions apparently dominated this region in the early to mid-1970s and also in the first 2–3 years of the 21st century. The similarities in south Patagonian precipitation records are not as strong as in the case of temperature records, and there is no long, regionally representative precipitation series to evaluate the variations of the last three to four decades in a 20th-century context. Based on the relationship between local precipitation and the ERA-Interim data, we reconstructed annual (April–March) total precipitation values since 1979 for Estancia Los Huemules, at the heart of the study area (Figs 1 and 9). This series shows that annual precipitation probably decreased over most of the 1979–2005 period, with only a minor recovery starting in 2002 (Fig. 7b). Although this

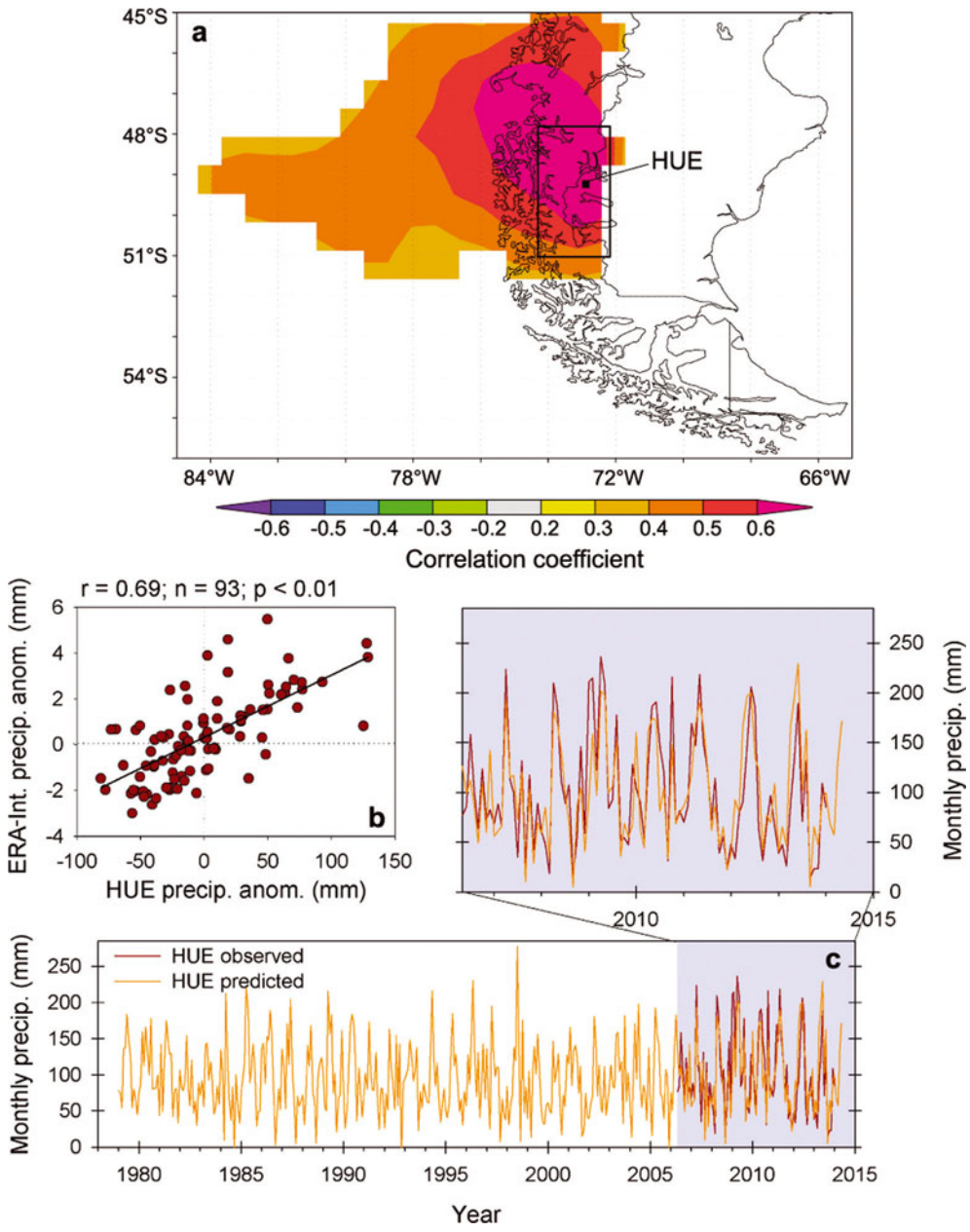

Fig. 9. (a) Field correlations between monthly precipitation anomalies between gridded ERA-Interim data and the precipitation recorded at Estancia Los Huemules (HUE) between 2006 and 2014. Only statistically significant correlations ($p < 0.05$) are shown. (b) Scatter plot showing the positive correlation between the precipitation anomalies of the HUE series and those of the ERA-Interim gridcell centered at 49° S, 73° W. (c) Monthly total variations recorded and predicted for HUE (dark red and orange, respectively). HUE monthly precipitation anomalies back to 1979 were first estimated through simple linear regression using the 49° S, 73° W ERA-Interim gridcell values as predictors, and then converted back to monthly total values by adding the seasonal cycle observed at HUE.

pattern is also consistent with the glacier reduction observed since 1979, it is clear that more detailed attribution assessments are needed to elucidate not only the climatic reasons for the observed glacier wastage but also to determine the relative influence of temperature vs precipitation on the long-term behavior of these glaciers (e.g. Marzeion and others, 2012).

6. CONCLUSIONS

Detailed, well-documented information on areal extent and measures of recent glacier changes in the south Patagonian Andes constitute important elements for the proper understanding of the current status of the cryosphere in this remote region. This information is relevant for studies of past and present glacier–climate relationships and complements current efforts for mapping and monitoring glaciers through national and international initiatives. In Argentina, the identification and inventory of Andean ice masses is currently well underway under the auspices of the National Glacier Inventory project. The results discussed in this paper are part of this project. Similar initiatives to inventory the Chilean glaciers are also being developed for adjacent basins in the Andes. Once completed, these initiatives (which include clean-ice but also debris-covered glaciers and rock glaciers) will constitute a major improvement and a historic landmark for the study and understanding of the cryospheric system in the southern Andes.

So far, most quantitative assessments of recent glacier changes in the southern Andes have relied on early aerial

photographs and/or archived Landsat satellite scenes as base images (e.g. Aniya 1988; Aniya and others, 1992, 1997; López and others, 2010). In this contribution we report promising results using declassified satellite photographs acquired by the Hexagon KH-9 US satellite (USGS, 2008; Fowler, 2013). These photographs cover significantly larger areas, and have substantially smaller inherent distortions, than traditional aerial photographs, requiring relatively little processing work and producing good co-registration with mid-resolution satellite scenes such as the ASTER images used here. Moreover, the pixel resolution (~10 m) of the KH-9 photographs is markedly smaller than contemporaneous Landsat images also available for this area, greatly improving the accuracy of the inventory maps that could eventually be developed using these photographs (e.g. Surazakov and Aizen, 2010).

The attribution of the possible climatic forcings behind the recent glacier shrinkage in the Patagonian Andes remains unclear. This is at least partly due to the lack of long, detailed glacio-meteorological measurements, which are difficult to obtain and maintain over long periods of time in this remote region. In this context, the identification and evaluation of new meteorological series from sites near glaciated areas in Patagonia is still highly relevant not only for testing climatic trends and patterns locally, but also for comparison and validation of larger-scale assessments of glacier variations derived from gridded datasets and modeling approaches (e.g. Willis and others, 2012; Lenaerts and others, 2014; Schaefer and others, 2015). In this study we show that ablation-season (October–March) temperatures measured between 2002 and 2012 in the study area are strongly and positively correlated with gridded reanalysis surface temperature data in southern Patagonia and also with the few official records available in this region (Fig. 6a). This is promising evidence that supports the use of gridded reanalysis data and/or distant station records to estimate and extend back in time the monthly and seasonal temperature variations in this and other glaciated areas in southern Patagonia. Unfortunately, precipitation records in this region are significantly shorter than temperature records and show more restricted areas of co-variability with gridded reanalysis data. This complicates the development of reliable precipitation records to estimate changes in accumulation in south Patagonian glaciers, and highlights the need to improve the network of glaciological and meteorological measurements in this remote region.

ACKNOWLEDGEMENTS

This work was funded by Consejo Nacional de Investigaciones Científicas y Técnicas (CONICET) and Agencia Nacional de Promoción Científica y Técnica (grants PICT 2007-0379 and PICT 2010-1438). We gratefully acknowledge the IGS for financial support, and the GLIMS project for enabling free access to ASTER satellite imagery. We are also grateful to the Technical Cooperation Program of the Japan International Cooperation Agency (JICA) and the Japan Aerospace Exploration Agency (JAXA) for providing additional funding and ALOS images. The ASTER, Landsat and KH-9 Hexagon data were obtained through the US Geological Survey (USGS) Earth Explorer website (http://earthexplorer.usgs.gov). ERA-Interim reanalysis data and correlation maps were provided by the freely available Climate Explorer online application maintained by Geert Jan van Oldenborgh at the Royal Netherlands Meteorological Institute (KNMI; http://climexp.knmi.nl/). E. Berthier acknowledges support from the French Space Agency (CNES) through his TOSCA program. Darío Trombotto and Daniel Falaschi (IANIGLA–CONICET) helped with the identification of rock glaciers. Helen Fricker (Scientific Editor), Graham Cogley and two anonymous reviewers provided detailed comments and suggestions that greatly improved the manuscript.

REFERENCES

Aniya M (1988) Glacier inventory for the Northern Patagonia Icefield, Chile, and variations 1944/45 to 1985/86. *Arct. Alp. Res.*, **20**(2), 179–187

Aniya M (2001) Glacier variations of Hielo Patagónico Norte, Chilean Patagonia, since 1944/45, with special reference to variations between 1995/96 and 1999/2000. *Bull. Glacier Res.*, **18**, 55–63

Aniya M, Naruse R, Shizukuishi M, Skvarca P and Casassa G (1992) Monitoring recent glacier variations in the Southern Patagonian Icefield, utilizing remote sensing data. *Int. Arch. Photogramm. Remote Sens.*, **29**(B7), 87–94

Aniya M, Sato H, Naruse R, Skvarca P and Casassa G (1996) The use of satellite and airborne imagery to inventory outlet glaciers of the Southern Patagonia Icefield, South America. *Photogramm. Eng. Remote Sens.*, **62**(12), 1361–1369

Aniya M, Sato H, Naruse R, Skvarca P and Casassa G (1997) Recent glacier variations in the Southern Patagonia Icefield, South America. *Arct. Alp. Res.*, **29**(1), 1–12

Aravena J-C and Luckman BH (2009) Spatio-temporal rainfall patterns in Southern South America. *Int. J. Climatol.*, **29**(14), 2106–2120 (doi: 10.1002/joc.1761)

Barsch D (1996) *Rock glaciers: indicators for the present and former geoecology in high mountain environments*. (Series in the Physical Environment 16) Springer, Berlin.

Bertone M (1960) *Inventario de los glaciares existentes en la vertiente Argentina entre los paralelos 47°30′ y 51° S*. Instituto Nacional del Hielo Continental Patagónico, Buenos Aires

Carrasco J, Casassa G and Rivera A (2002) Meteorological and climatological aspects of the Southern Patagonia Icefield. In Casassa G, Sepúlveda FV and Sinclair RM eds. *The Patagonian Icefields: a unique natural laboratory for environmental and climate change studies*. Kluwer Academic/Plenum Publishers, New York

Casassa G, Sepúlveda FV and Sinclair RM eds (2002) *The Patagonian Icefields: a unique natural laboratory for environmental and climate change studies*. Kluwer Academic/Plenum Publishers, New York

Davies BJ and Glasser NF (2012), Accelerating shrinkage of Patagonian glaciers from the Little Ice Age (~AD 1870) to 2011. *J. Glaciol.*, **58**(212), 1063–1084 (doi: 10.3189/2012JoG12J026)

Dee DP and 35 others (2011) The ERA-Interim reanalysis: configuration and performance of the data assimilation system. *Q. J. R. Meteorol. Soc.*, **137**, 553–597

Falaschi D, Bravo C, Masiokas MH, Villalba R and Rivera A (2013) First glacier inventory and recent changes in glacier area in the Monte San Lorenzo region (47° S), southern Patagonian Andes, South America. *Arct. Antarct. Alp. Res.*, **45**(1), 19–28

Fowler MJF (2013) Declassified Intelligence Satellite Photographs. In Hanson WS and Oltean IA eds *Archaeology from historical aerial and satellite archives*. Springer Science+Business Media, Berlin, 47–66 (doi: 10.1007/978-1-4614-4505-0_4)

Frey H and Paul F (2012) On the suitability of the SRTM DEM and ASTER GDEM for the compilation of topographic parameters in glacier inventories. *Int. J. Appl. Earth Obs. Geoinf.*, **18**, 480–490 (doi: 10.1016/j.jag.2011.09.020)

Garreaud R, Lopez P, Minivielle M and Rojas M (2013) Large scale control on the Patagonian climate. *J. Climate,* **26**(1), 215–230 (doi: 10.1175/jcli-d-12-00001.1

Hollingsworth J, Leprince S, Ayoub F and Avouac JP (2012) Deformation during the 1975–1984 Krafla rifting crisis, NE Iceland, measured from historical optical imagery. *J. Geophys. Res: Solid Earth*, **117**(B11), B11407 (doi: 10.1029/2012JB009140)

IANIGLA (2010) *Inventario Nacional de Glaciares y Ambiente Periglacial: Fundamentos y Cronograma de Ejecución*. Instituto Argentino de Nivología, Glaciología y Ciencias Ambientales–Consejo Nacional de Investigaciones Científicas y Técnicas (IANIGLA–CONICET), Buenos Aires

Kölliker A, Kühn F, Reichert A, Tomsen A and Witte L (1917) *Patagonia: resultados de las expediciones realizadas en 1910 a 1916*, 2 vols. Sociedad Científica Alemana, Buenos Aires

Lenaerts JTM and 6 others (2014) Extreme precipitation and climate gradients in Patagonia revealed by high-resolution regional atmospheric climate modeling. *J. Climate*, **27**, 4607–4621

Leprince S, Barbot S, Ayoub F and Avouac JP (2007) Automatic and precise orthorectification, coregistration, and subpixel correlation of satellite images: application to ground deformation measurements. *IEEE Trans. Geosci. Remote Sens.*, **45**(6), 1529–1558

Lliboutry L. (1953) More about advancing and retreating glaciers in Patagonia. *J. Glaciol.*, **2**(13), 168–172

López P, Chevallier P, Favier V, Pouyaud B, Ordenes F and Oerlemans J (2010) A regional view of fluctuations in glacier length in southern South America. *Global Planet. Change*, **71**, 85–108

Marzeion B, Hofer M, Jarosch AH, Kaser G and Molg T (2012) A minimal model for reconstructing interannual mass balance variability of glaciers in the European Alps. *Cryosphere*, **6**, 71–84 (doi: 10.5194/tc-6-71-2012)

Masiokas, MH, Luckman B, Villalba R, Delgado S, Skvarca P and Ripalta A (2009a) Little Ice Age fluctuations of small glaciers in the Monte Fitz Roy and Lago del Desierto areas, south Patagonian Andes, Argentina. *Palaeogeogr. Palaeoclimatol. Palaeoecol.*, **281**(3–4), 351–362

Masiokas MH, Rivera A, Espizua LE, Villalba R, Delgado S and Aravena JC (2009b) Glacier fluctuations in extratropical South America during the past 1000 years. *Palaeogeogr. Palaeoclimatol. Palaeoecol.*, **281** (3–4), 242–268

Mercer JH (1965) Glacier variations in Southern Patagonia. *Geogr. Rev.*, **55**, 390–413

Pfeffer WT and 65 others (2014) The Randolph Glacier Inventory: a globally complete inventory of glaciers. *J. Glaciol.* **60**(221), 537–552 (doi: 10.3189/2014JoG13J176)

Pieczonka T, Bolch T, Junfeng W and Shiyin L (2013) Heterogeneous mass loss of glaciers in the Aksu-Tarim Catchment (Central Tien Shan) revealed by 1976 KH-9 Hexagon and 2009 SPOT-5 stereo imagery. *Remote Sens. Environ.*, **130**(213), 233–244 (doi: 10.1016/j.rse.2012.11.020)

Popovnin VV, Danilova TA and Petrakov DA (1999) A pioneer mass balance estimate for a Patagonian glacier: Glaciar De los Tres, Argentina. *Global Planet. Change*, **22**(1), 255–267

Racoviteanu, AE, Paul F, Raup B, Khalsa SJS and Armstrong R (2009) Challenges and recommendations in mapping of glacier parameters from space: results of the 2008 Global Land Ice Measurements from Space (GLIMS) workshop, Boulder, Colorado, USA. *Ann. Glaciol.*, **50**(53), 53–69.

Rasmussen L, Conway H and Raymond C (2007) Influence of upper air conditions on the Patagonia Icefields. *Global Planet. Change*, **59**, 203–216

Rignot E, Rivera A and Cassasa G (2003) Contribution of the Patagonia Icefields of South America to sea level rise. *Science*, **302**(5644), 434–437

Rosenblüth B, Casassa G and Fuenzalida H (1995) Recent climatic changes in western Patagonia. *Bull. Glacier Res.*, **13**, 127–132

Rosenblüth B, Fuenzalida H and Aceituno P (1997) Recent temperature variations in southern South America. *Int. J. Climatol.*, **17**, 67–85

Röthlisberger F (1986) *10,000 Jahre Gletschergeschichte der Erde*. Verlag Sauerländer, Aarau

Schaefer M, Machguth H, Falvey M and Casassa G (2013) Modeling past and future surface mass balance of the Northern Patagonia Icefield. *J. Geophys. Res.*, **118**, 571–588 (doi: 10.1002/jgrf.20038)

Schaefer M, Machguth H, Flavey M, Casassa G and Rignot E (2015) Quantifying mass balance processes on the Southern Patagonia Icefield. *Cryosphere*, **9**(1), 25–35 (doi: 10.5194/tc-9-25-2015)

Simmons AJ, Willett KM, Jones PD, Thorne PW and Dee DP (2010) Low-frequency variations in surface atmospheric humidity, temperature and precipitation: inferences from reanalyses and monthly gridded observational datasets. *J. Geophys. Res.*, **115**(D1), D01110 (doi: 10.1029/2009JD012442)

Skvarca P and De Angelis H (2003) First cloud-free Landsat TM image mosaic of Hielo Patagónico Sur, southwestern Patagonia, South América. (Contribución No. 535) Dirección Nacional del Antártico–Instituto Antártico Argentino, Buenos Aires

Surazakov AB and Aizen VB (2010) Positional accuracy evaluation of declassified Hexagon KH-9 mapping camera imagery. *Photogramm. Eng. Remote Sens.*, **76**(5), 603–608

Tadono T, Shimada M, Murakami H and Takaku J (2009) Calibration of PRISM and AVNIR-2 onboard ALOS 'Daichi'. *IEEE Trans. Geosci Remote Sens.*, **47**(12-1), 4042–4050

US Geological Survey (USGS) (2008) Declassified intelligence satellite photographs. USGS Fact Sheet 2008-3054 http://pubs.usgs.gov/fs/2008/3054/

Villalba R and 9 others (2003) Large-scale temperature changes across the southern Andes: 20th-century variations in the context of the past 400 years. *Climatic Change*, **59**(1–2), 177–232

Warren CR and Sugden DE (1993) The Patagonian icefields: a glaciological review. *Arct. Alp. Res.*, **25**, 316– 331

Willis MJ, Melkonian AK, Pritchard ME and Rivera A (2012) Ice loss from the Southern Patagonian Ice Field, South America, between 2000 and 2012. *Geophys. Res. Lett.*, **39**(17), L17501 (doi: 10.1029/2012GL053136)

Zalazar L and 12 others (2012) An updated glacial and periglacial inventory of the Río Mendoza basin in the Central Andes of Argentina (1:250,000). In World Glacier Monitoring Service, *Fluctuations of glaciers 2005–2010 (Vol. X)*, ed. Zemp M and 6 others. ICSU (FAGS)/IUGG (IACS)/UNEP/UNESCO/WMO, World Glacier Monitoring Service, Zürich, 2–58. http://www.wgms.ch/fog/wgms_2012_fogX.pdf

MS received 13 May 2014 and accepted in revised form 10 April 2015